International Journal of Minerals, Metallurgy and Materials
Volume 21, Number 4, April 2014, Page 331
DOI: 10.1007/s12613-014-0913-x

Distribution behavior of phosphorus in the coal-based reduction of high-phosphorus-content oolitic iron ore

Yong-sheng Sun, Yue-xin Han, Peng Gao, and Duo-zhen Ren

College of Resources and Civil Engineering, Northeastern University, Shenyang 110819, China
(Received: 3 September 2013; revised: 23 October 2013; accepted: 28 October 2013)

Abstract: This study focuses on the reduction of phosphorus from high-phosphorus-content oolitic iron ore via coal-based reduction. The distribution behavior of phosphorus (i.e., the phosphorus content and the phosphorus distribution ratio in the metal, slag, and gas phases) during reduction was investigated in detail. Experimental results showed that the distribution behavior of phosphorus was strongly influenced by the reduction temperature, the reduction time, and the C/O molar ratio. A higher temperature and a longer reaction time were more favorable for phosphorus reduction and enrichment in the metal phase. An increase in the C/O ratio improved phosphorus reduction but also hindered the mass transfer of the reduced phosphorus when the C/O ratio exceeded 2.0. According to scanning electron microscopy analysis, the iron ore was transformed from an integral structure to metal and slag fractions during the reduction process. Apatite in the ore was reduced to P, and the reduced P was mainly enriched in the metal phase. These results suggest that the proposed method may enable utilization of high-phosphorus-content oolitic iron ore resources.

Keywords: iron ores; phosphorus; ore reduction; pyrometallurgy

1. Introduction

The high-phosphorus-content oolitic iron ore in China is a typical high-phosphorus-content (with an average phosphorus content of 0.8wt%) iron ore resource with a large reserve of 3.72×10^9 t. Between the 1960s and 1970s, investigations on the processing of oolitic hematite started in China, and various possible mineral separation methods have been explored. However, no satisfactory mineral processing methods have been developed because of the low grade of the iron ore (35wt% to 50wt% Fe), the poor liberation of iron minerals, the high phosphorous content, and so on [1–3]. The high-phosphorus-content oolitic hematite ore is considered to be one of the most refractory iron ores.

With the rapid development of its iron and steel industry, China has emerged as the largest steel producer in the world for ten consecutive years. Thus, China has intensified its focus on the utilization of refractory iron ores (especially oolitic iron ore). Numerous studies on the recovery of iron from high-phosphorus-content oolitic iron ore have been published, and the results suggest that direct reduction followed by magnetic separation is the most effective technique [2–8]. However, the considerable amount of phosphorus in the ore that transfers into metallic iron during direct reduction poses a serious problem [9]. Studies have focused on the removal of phosphorus from high-phosphorus-content iron ore through the addition of a dephosphorization agent during the reduction process [10−11]. However, high quantities of dephosphorization agent are needed due to the high phosphorus content in the ore, which results in an expensive reduction process and the inability to recover phosphorous from the ore.

Phosphorus is one of the most detrimental impurities in steels, and most of phosphorus in metallic iron phase is eliminated into the steelmaking slag [12–13]. However, the concentration of P_2O_5 in these slags is typically 1wt% to 3wt%, which makes it ineffective as a fertilizer or phosphorus resource [14]. A previous study has indicated that the duplex steelmaking process developed in Japan is favorable to dephosphorization [12, 15]. In the case of a normal hot metal ([P] = 0.1wt%), the P_2O_5 content in the dephosphori-

Corresponding author: Yue-xin Han E-mail: dongdafulong@mail.neu.edu.cn

zation slag is approximately 5wt%. When the phosphorus concentration in the hot metal is adjusted to between 0.15wt% and 0.25wt%, the P_2O_5 content in the slag exceeds 10wt% [12]. Hence, we proposed a new method that enables the possible comprehensive exploitation of high-phosphorus-content oolitic iron ore. Phosphorus in the iron ore will be forced to migrate into the metallic iron phase during the reduction process, which allows the collection of reduced iron powder with high phosphorus content by magnetic separation. The high-phosphorus reduced iron powder is then refined by a duplex steelmaking process. Afterward, molten steel is produced, and high-phosphorus-content steelmaking slag that can be used as a phosphate fertilizer is also obtained. The migration characteristics of phosphorus and the phosphorus content in the metallic iron phase are the key points to this method.

With this background, we here report the results of our research into the distribution behavior of phosphorus (i.e., the phosphorus content in the slag and metal phases as well as the phosphorus distribution ratio in the metal, slag, and gas phases). In addition, the microstructure and composition characteristics of reduced products were studied. The present study aims to provide a basis for the rational utilization of high-phosphorus-content oolitic iron ore.

2. Thermodynamic basis for phosphorus reduction

In the iron ore, phosphorus usually exists as apatite, which is a double salt formed by $Ca_3(PO_4)_2$ and CaF_2, $CaCl_2$, or $Ca(OH)_2$, and $Ca_3(PO_4)_2$ is the main component. According to the Ellingham diagram [16], the lines for the reactions $4/5P + O_2 = 2/5P_2O_5$ and $6FeO + O_2 = 2Fe_3O_4$ are close to each other. Hence, phosphorus is almost reduced in the blast furnace during iron making and transfers into the hot metal.

During reduction, calcium phosphate can be reduced to P by carbon. SiO_2 can displace P_2O_5 in calcium phosphate, and P_2O_5 is then reduced by carbon. Therefore, the reaction of calcium phosphate can be accelerated. The reaction mechanism of calcium phosphate to P can be expressed by the following reactions:

$$Ca_3(PO_4)_2(s) + 5C(s) = 3CaO(s) + 2[P] + 5CO(g) \quad (1)$$

$$1/3Ca_3(PO_4)_2(s) + SiO_2(s) + 5/3C(s) = CaO{\cdot}SiO_2(s) + 2/3[P] + 5/3CO(g) \quad (2)$$

$$Ca_3(PO_4)_2(s) + 2SiO_2(s) + 5C(s) = 3CaO{\cdot}2SiO_2(s) + 2[P] + 5CO(g) \quad (3)$$

$$2/3Ca_3(PO_4)_2(s) + SiO_2(s) + 10/3C(s) = 2CaO{\cdot}SiO_2(s) + 4/3[P] + 10/3CO(g) \quad (4)$$

The calculated thermodynamic results for reactions (1) to (4) are exhibited in Fig. 1 to reflect the relationship between the standard Gibbs energies ($\Delta G^{\ominus}$) and the temperature. The initial temperatures at atmospheric pressure at which reactions (1), (2), (3), and (4) will occur are 1495, 1224, 1269, and 1287°C, respectively. In addition, the standard Gibbs free energies of these reactions significantly decrease with increasing temperature, which demonstrates that calcium phosphate is more easily reduced at high temperatures.

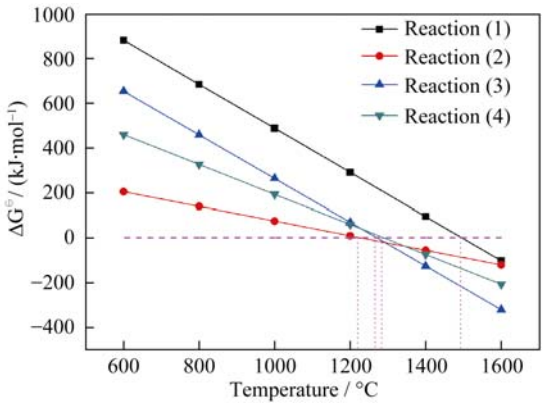

Fig. 1. Correlation between $\Delta G^{\ominus}$ and temperature for reactions (1) to (4).

In this study, the reduction temperature ranged from 1175 to 1275°C, which is close to (or above) the initial temperatures of reactions (2) to (4). Thus, the partial apatite in the ore is reduced to P. Because the reduction process was performed in an open $MoSi_2$ muffle resistance furnace, the small amount of P reduced from the apatite will volatilize into the gas phase and the nonvolatilized portion will migrate into the metal phase. The unreduced apatite and some P atoms that have not yet migrated into metallic iron will remain in the slag phase. These analyses indicate that apatite in the iron ore can be reduced using coal-based reduction and that phosphorus will be present in the metal, slag, and gas phases after the reduction process.

3. Experimental

3.1. Materials

The representative samples of high-phosphorus-content oolitic iron ore were collected from the Guandian Iron Mine, Hubei Province, China. A total of 1 t ore was collected. The ore was then crushed, classified, homogenized, and sampled. The final sample had a particle size of 100% passing 2 mm, and its chemical composition is shown in Table 1. The results indicate that the contents of total iron, SiO_2, Al_2O_3, and CaO were approximately 42.21wt%, 21.80wt%, 5.47wt%, and 4.33wt%, respectively, whereas the content of harmful phosphorus was relatively high at 1.31wt%. The ore was

mainly composed of iron oxides and silicates. The mineralogical analysis of the iron ore sample was performed using X-ray diffraction (XRD). The main crystalline phases were hematite, quartz, chamosite, and apatite (Fig. 2).

Table 1. Chemical composition of high-phosphorus-content oolitic iron ore wt%

Fe_{total}	FeO	SiO_2	Al_2O_3	CaO	MgO	P	S	TiO_2	K	Mn
42.21	4.31	21.80	5.47	4.33	0.59	1.31	0.13	0.19	0.41	0.20

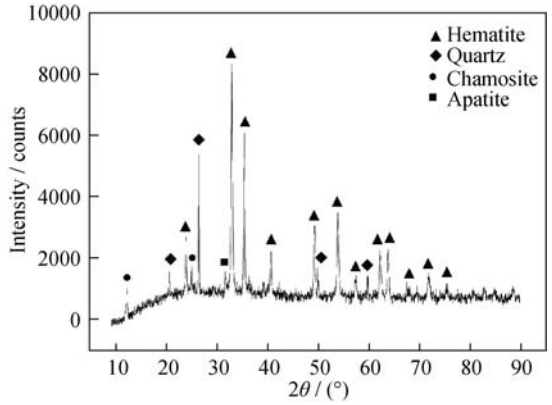

Fig. 2. XRD pattern of the oolitic iron ore.

The SEM image of the sample is illustrated in Fig. 3, in which the ooid structure can be readily observed. Thus, the iron ore was a typical oolitic iron ore. Hematite was most predominant in the image, followed by quartz. This result also indicates that hematite was the most important iron mineral in the ore and that the primary silicate mineral was quartz. Apatite was the only phosphate mineral and usually appeared as oolitic layers; the phosphate was mainly associated with hematite. The details of apatite in the ooid were investigated by line-by-line scanning; the results are shown in Fig. 4. The distribution of P was identical to that of Ca and alternated with Fe. This result further shows that apatite is closely associated with hematite in the ore.

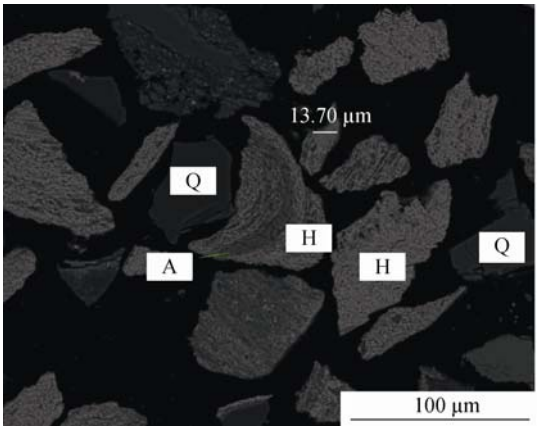

Fig. 3. SEM image of the ore sample: A—apatite; Q—quartz; H—hematite.

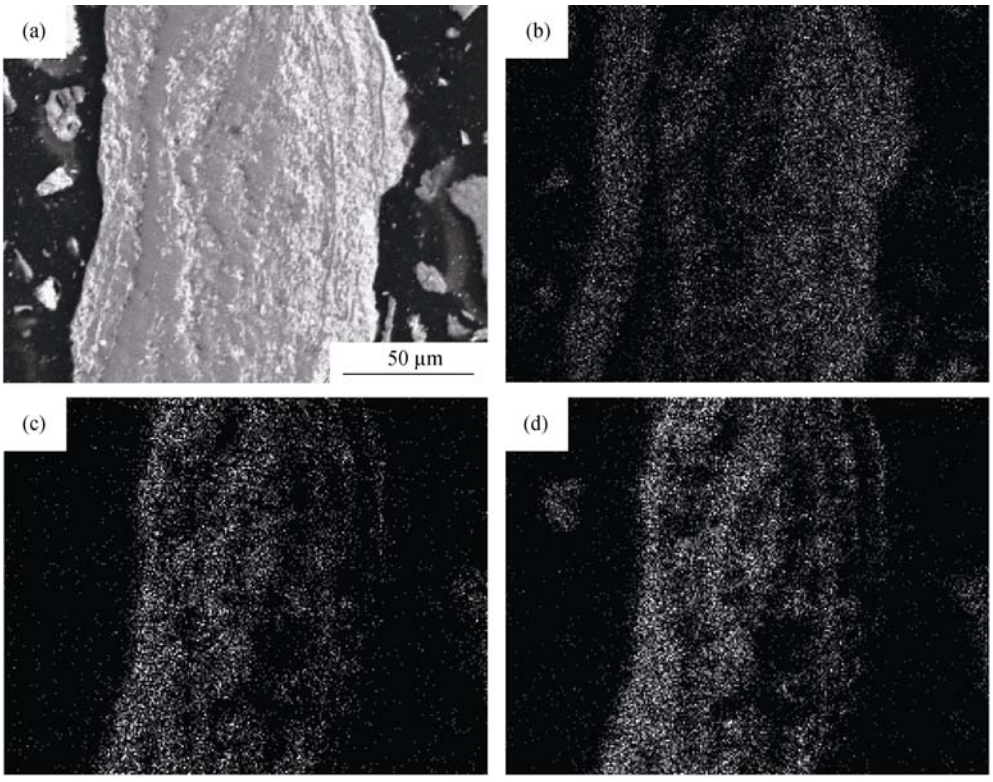

Fig. 4. Line-by-line scanning images of the ooid structure: (a) image of selected area; (b) Fe; (c) P; (d) Ca.

An anthracite coal that was crushed to 100% passing 2 mm was used as a reductant. The proximate analysis results of the coal are listed in Table 2 and indicate that the coal contains a high content of fixed carbon and comparatively low content of ash, volatiles, sulfur, and phosphorus. The coal is therefore a good reducing agent for coal-based reduction.

Table 2. Proximate analysis of the coal wt%

FC_d	V_d	A_d	M_{ad}	P	S
67.83	18.45	12.02	1.48	0.004	0.028

Note: M_{ad}—moisture; A_d—ash; V_d—volatile matter; FC_d—fixed carbon.

3.2. Experimental method

Three main factors that influence the distribution of phosphorus were investigated on the basis of the characteristics of coal-based reduction. These parameters are the reduction temperature, the reduction time, and the C/O molar ratio (i.e., the molar ratio of fixed carbon in the coal to reducible oxygen in iron oxides). The iron ore samples and the coal were thoroughly mixed in specific proportions by rigorous stirring for approximately 30 min. The prepared mixtures were then reduced at various temperatures and time in an open special $MoSi_2$ furnace (Fig. 5), in which the temperature fluctuation was controlled to within 1.5°C. Coal was placed at both the inlet and outlet sides of the furnace to ensure that a reducing atmosphere was present within the furnace. After the reduction process, the reduced samples were rapidly removed and immediately quenched in water, filtered, and dried at 80°C in a vacuum oven. In addition, purge gases were not utilized during the reduction and the reduction experiments were run at atmospheric conditions.

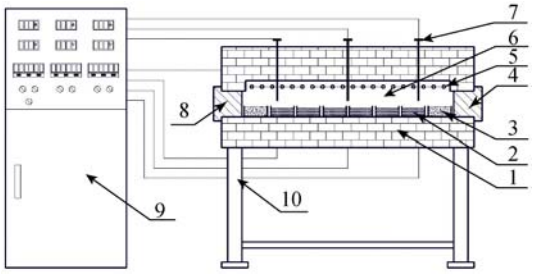

Fig. 5. Schematic diagram of the reduction apparatus: 1—furnace; 2—prepared mixtures; 3—coal; 4—outlet; 5—$MoSi_2$ heating element; 6—hearth; 7—thermocouple for temperature measurement; 8—inlet; 9—control cabinet; 10—bed.

The metallic iron content in the reduced samples was determined by titrimetry. The phosphorus content in the metals and slag were measured by spectrophotometry and X-ray fluorescence spectrometry, respectively. The phosphorus distribution ratios in the metal, slag, and gas phases are defined by Eqs. (5), (6), and (7), respectively:

$$P_{dm} = P_m \times m_m / (P_o \times m_o) \times 100\% \quad (5)$$

$$P_{ds} = P_s \times m_s / (P_o \times m_o) \times 100\% \quad (6)$$

$$P_{dg} = 1 - P_{dm} - P_{ds} \quad (7)$$

where P_{dm} is the P distribution ratio in the metal phase, P_m is the P content in the metal, m_m is the mass of the metal in the reduced sample, P_o is the P content in the ore sample, m_o is the mass of the ore sample in the mixture, P_{ds} is the P distribution ratio in the slag phase, P_s is the P content in the slag, m_s is the mass of the slag in the reduced sample, and P_{dg} is the P distribution ratio in the gas phase.

The morphology and microstructure of the reduced sample was studied using a SSX-550 scanning electron microscope (SHIMADZU). The composition was analyzed by energy-dispersive spectrometry (EDS) on an Inca X-ray spectrometer combined with the scanning electron microscope.

4. Results and discussion

4.1. Distribution behavior of phosphorus

4.1.1. Effect of reduction temperature

The ore samples were reduced at temperatures between 1175 and 1275°C to determine the effect of temperature on the distribution behavior of phosphorus. The results are illustrated in Fig. 6. The data reveal that the reduction temperature significantly affected the distribution behavior of phosphorus. Both the phosphorus content in the metal and the P_{dm} rapidly increased when the temperature was increased from 1175 to 1275°C. Conversely, a sharp decrease in the P_{ds} and the phosphorus content of the slag was observed. The P_{dg} gradually increased as the reduction temperature was increased and then leveled off after the reduction temperature reached 1250°C. The results can be derived from thermodynamic data in Fig. 1, in which the $\Delta G^{\ominus}$ values of reactions (1) to (4) decrease as the temperature increases. This phenomenon demonstrates that the reduction reactions (1) to (4) can be improved through an increase in temperature. Therefore, more apatite in the ore was reduced to P at higher temperatures. Meanwhile, when the reduction temperature is increased, the diffusion coefficient of P will significantly increase, which will accelerate the enrichment of P in the metal and gas phases.

4.1.2. Effect of reduction time

A series of experiments were conducted at various reduction time to determine their effect on the distribution behavior of phosphorus. The effect of reduction time on the phosphorus content in the metal and slag is plotted in Fig.

7(a). The phosphorus content increased in the metal but decreased in the slag as the reduction time was increased. The phosphorus distribution ratios in the metal, slag, and gas phases as functions of reduction time are shown in Fig. 7(b). When the reduction time was increased, the phosphorus distribution ratios in both the metal and gas increased, whereas the phosphorus distribution ratio in the slag decreased. This phenomenon was consistent with the changes in the phosphorus contents in the metal and slag. After the maximum reduction time (70 min), the phosphorus content was as high as 2.14wt% in the metal and as low as 0.314wt% in the slag. The phosphorus distribution reached 70.08% and 16.21% in the reduced metals and the slag, respectively. This phenomenon occurs because more apatite in the ore is reduced and more reduced P migrates into the metal phase as the reduction time is extended.

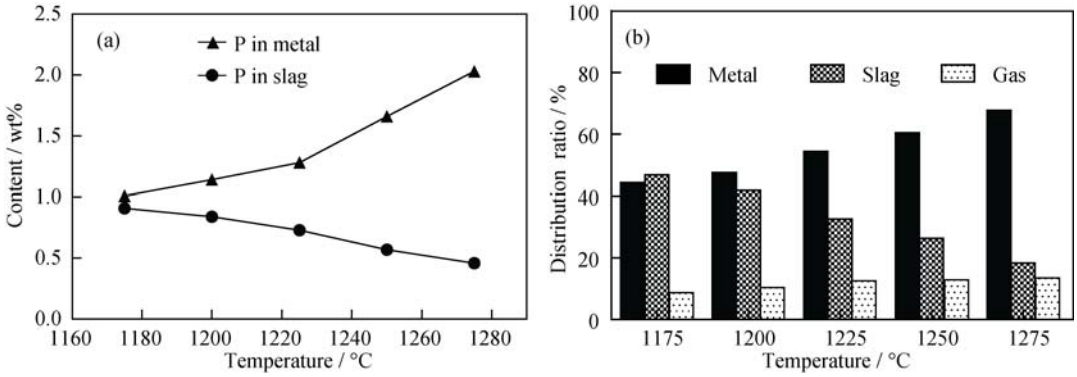

Fig. 6. Effect of reduction temperature on the distribution behavior of phosphorus (C/O molar ratio of 2.5; reduction time of 50 min): (a) phosphorus content; (b) distribution ratio.

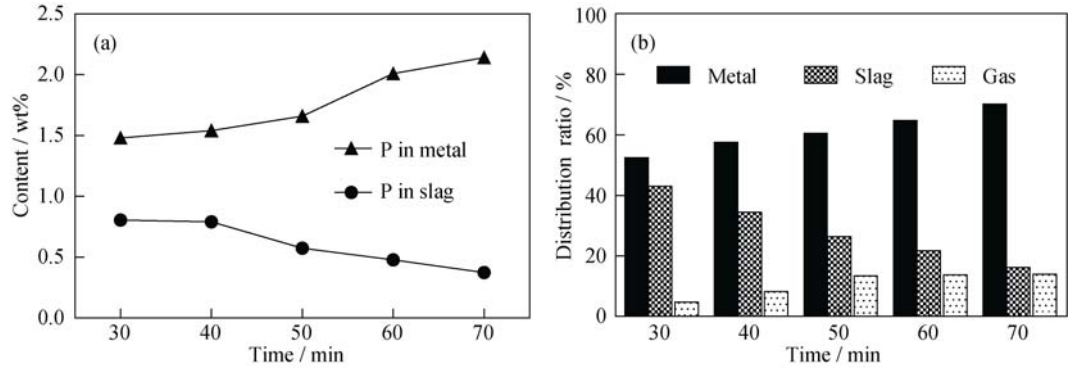

Fig. 7. Effect of reduction time on the distribution behavior of phosphorus (C/O molar ratio of 2.5; reduction at 1250°C): (a) phosphorus content; (b) distribution ratio.

4.1.3. Effect of the C/O molar ratio

The effect of the C/O molar ratio (i.e., the molar ratio between the fixed carbon in the coal and the reducible oxygen in the ore) on the distribution behavior of phosphorus was studied at C/O values that varied from 1.0 to 3.0 (Fig. 8). The distribution behavior of phosphorus was considerably affected by the amount of reductant. The phosphorus content in the metal increased with increasing C/O ratio and decreased when the C/O ratio exceeded 2.0. The changes in the P_{dm} as a function of the C/O ratio were consistent with the phosphorus content in the metal. This phenomenon is attributed to more reductant promoting the reduction of phosphorus but also hindering the migration of the reduced P into the metal phase. Both the phosphorus content in the slag and the P_{ds} substantially decreased and then slightly decreased when the C/O ratio was greater than 2.0. The P_{dg} increased with increasing C/O ratios (Fig. 8(b)) because the content of volatile matter increases with the increase of the amount of reductant and more reduced phosphorus will volatilize into gas with the volatile matter.

4.2. Characterization of the reduced sample

4.2.1. Phase composition of the reduced sample

The XRD pattern of a selected reduced sample is shown in Fig. 9. The XRD pattern shows that iron appeared most often in the form of metallic iron in the reduced sample; metallic iron is easily recovered by low-intensity magnetic separation after it has been liberated. SiO_2 was still the pri-

mary impurity. However, in comparison with the XRD pattern of the original iron ore (as shown in Fig. 2), the pattern of the reduced sample contains no apatite peaks, which reveals that apatite did react with the reductant during the reduction process. Moreover, the peaks of SiO_2 became less intense, and the peaks of chamosite disappeared after the reduction process. Peaks attributable to Ca_2SiO_4 and $Ca(Al_2Si_2O_8)$ appeared in the XRD pattern of the reduced sample, which indicates that SiO_2 and chamosite in the ore had reacted during the reduction process.

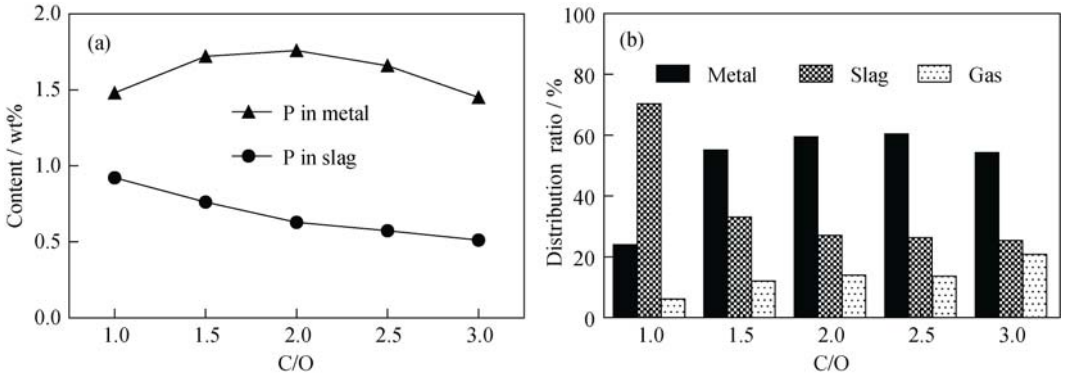

Fig. 8. Effect of C/O molar ratio on the distribution behavior of phosphorus (reduction at 1250°C for 50 min): (a) phosphorus content; (b) distribution ratio.

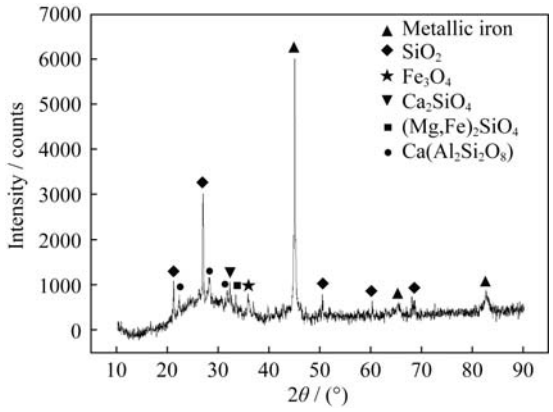

Fig. 9. XRD pattern of the reduced sample (C/O molar ratio of 2.0, reduction at 1250°C for 50 min).

4.2.2. SEM analysis of the reduced sample

We also investigated the selected sample by SEM to better understand the previously discussed experimental results. The SEM images of the reduced sample and the results of EDS measurements at different points and of surface scans of Fe, O, P, and Ca are illustrated in Fig. 10. The SEM images of the original ore and reduced samples showed that iron minerals in the ore were reduced to metallic iron and that the metal set in the slag in the form of spherical particles (Fig. 3 and Fig. 10). The complicated particles of high-phosphorus-content oolitic iron ore changed in the metal and slag phases after reduction. On the basis of the EDS analyses of spots 1 and 2, P exists in the metal phase and the slag is mainly composed of Si, Al, P, Ca, and O. These results demonstrate that apatite in the ore was reduced to P and that the reduced P transferred to the metallic iron phase during the reduction process. According to the line-by-line scanning results of the reduced sample, the distribution of P clearly coincided with Fe, whereas Ca was scattered in the space of P, which further indicated that apatite was reduced to P and that the reduced P was enriched in the metal phase.

5. Conclusions

The reduction of phosphorus in high-phosphorus-content oolitic iron ore was examined using coal-based reduction. The effects of reduction temperature, reduction time, and coal content on the distribution behavior of phosphorus were investigated. The results are summarized as follows.

(1) Reduction temperature, reduction time, and coal content significantly influenced the distribution behavior of phosphorus. Both the phosphorus content and the distribution ratio in the metal phase increased with increasing reaction temperature and time. The phosphorus content and distribution ratio in the slag phase decreased with an increase in the three aforementioned factors, while those in the gas phase increased. With an increase in the C/O ratio, the phosphorus content and the distribution ratio in the metal initially increased, but decreased when the C/O ratio exceeded 2.0.

(2) During the reduction process, the original ore sample was reduced to the metal and slag phases. Apatite was reduced to P, and most of the reduced P enriched into the metal, with a small amount of P volatilized into the gas phase. The unreduced apatite and some reduced P that did not migrate into the metal phase were retained in the slag phase.

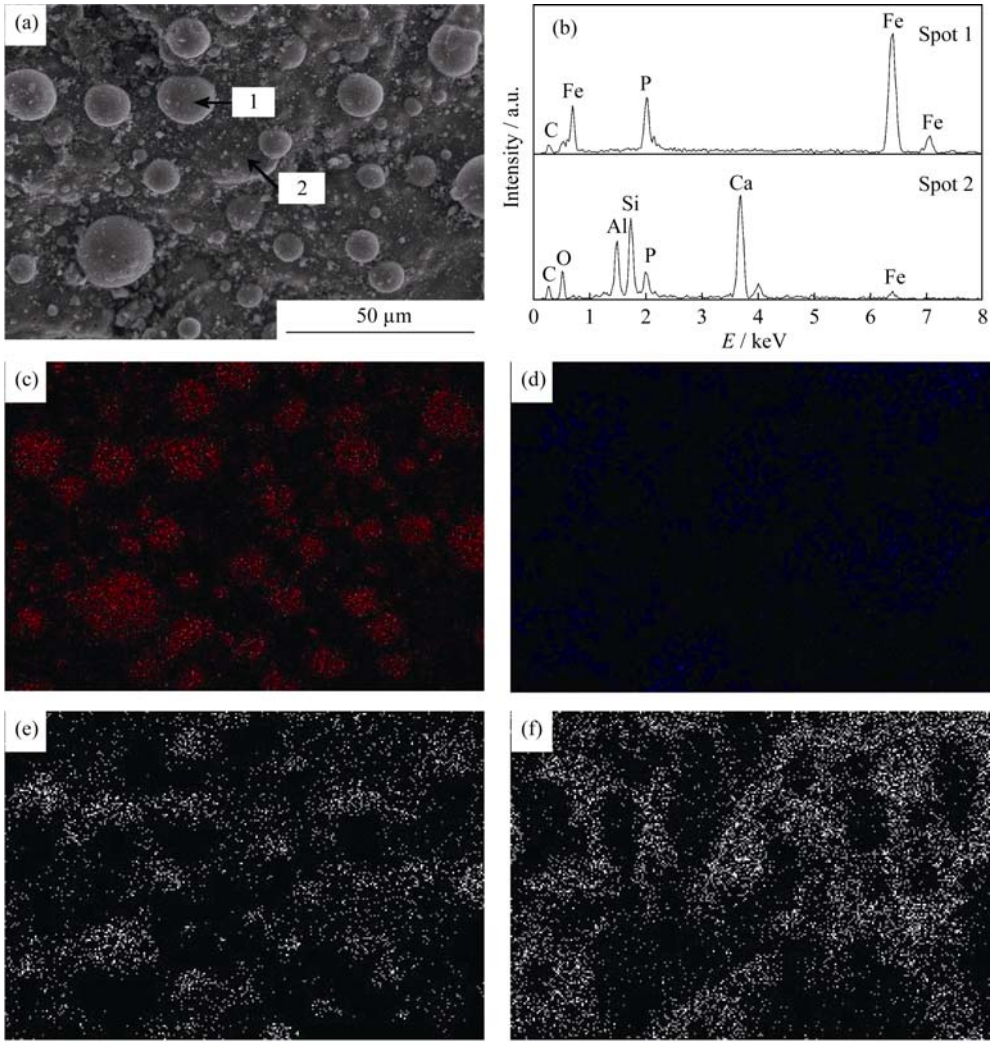

Fig. 10. SEM analysis results of the reduced sample (C/O molar ratio of 2.0, reduction at 1250°C for 50 min): (a) image of selected area; (b) EDS spectra; (c) Fe; (d) O; (e) P; (f) Ca.

(3) For all the experiments, the phosphorus content in the metal phase was greater than 1.0wt%. Therefore, when the reduced iron powder (which can be separated by magnetic separation) is refined by a duplex steelmaking process, a slag that contains more than 10wt% P_2O_5 will be obtained. This slag can be used as a fertilizer or as a phosphorus resource. Our analysis demonstrates that the recovery of phosphorus from high-phosphorus-content oolitic iron ore is feasible. The results of this study indicate that the rational utilization of high-phosphorus-content oolitic iron ore is possible.

Acknowledgements

This work was financially supported by the National Natural Science Foundation of China (No. 51134002) and the Fundamental Research Funds for the Central Universities of China (No. N120601004).

References

[1] Y.S. Sun, Y.X. Han, P. Gao, Z.H. Wang, and D.Z. Ren, Recovery of iron from high phosphorus oolitic iron ore using coal-based reduction followed by magnetic separation, *Int. J. Miner. Metall. Mater.*, 20(2013), No. 5, p. 411.

[2] S.F. Li, Y.S. Sun, Y.X. Han, G.Q. Shi, and P. Gao, Fundamental research in utilization of an oolitic hematite by deep reduction, *Adv. Mater. Res.*, 158(2011), p. 106.

[3] Y.S. Sun, P. Gao, Y.X. Han, and D.Z. Ren, Reaction behavior of iron minerals and metallic iron particles growth in coal-based reduction of an oolitic iron ore, *Ind. Eng. Chem. Res.*, 52(2013), No. 6, p. 2323.

[4] P. Gao, Y.S. Sun, D.Z. Ren, and Y.X. Han, Growth of metallic iron particles during coal-based reduction of a rare-earths-bearing iron ore, *Miner. Metall. Process.*, 30(2013), No. 1, p. 74.

[5] K.Q. Li, W. Ni, M. Zhu, M.J. Zheng, and Y. Li, Iron extraction from oolitic iron ore by a deep reduction process, *J. Iron*

Steel Res. Int., 18(2011), No. 8, p. 9.

[6] H.Q. Tang, Z.C. Guo, and Z.L. Zhao, Phosphorus removal of high phosphorus iron ore by gas-based reduction and melt separation, *J. Iron Steel Res. Int.*, 17(2010), No. 9, p. 1.

[7] Y.F. Yu and C.Y. Qi, Magnetizing roasting mechanism and effective ore dressing process for oolitic hematite ore, *J. Wuhan Univ. Technol. Mater. Sci. Ed.*, 26(2011), No. 2, p. 176.

[8] J. Wu, Z.J. Wen, and M.J. Cen, Development of technologies for high phosphorus oolitic hematite utilization, *Steel Res. Int.*, 82(2011), No. 5, p. 494.

[9] C.R. Manning and R.J. Fruehan, The behavior of phosphorus in direct-reduced iron and hot briquetted iron, *Iron Steelmaker*, 30(2003), p. 62.

[10] C.Y. Xu, T.C. Sun, C.Y. Qi, Y.L. Li, X.L. Mo, D.W. Yang, Z.X. Li, and B.L. Xing, Effects of reductants on direct reduction and synchronous dephosphorization of high-phosphorous oolitic hematite, *Chin. J. Nonferrous Met.*, 21(2011), No. 3, p. 680.

[11] D.W. Yang, T.C. Sun, H.F. Yang, C.Y. Xu, C.Y. Qi, and Z.X. Li, Dephosphorization mechanism in a roasting process for direct reduction of high-phosphorus oolitic hematite in west Hubei Province, China, *J. Univ. Sci. Technol. Beijing*, 32(2010), No. 8, p. 968.

[12] J. Diao, B. Xie, Y.H. Wang, and X. Guo, Recovery of phosphorus from dephosphorization slag produced by duplex high phosphorus hot metal refining, *ISIJ Int.*, 52(2012), No. 6, p. 955.

[13] H. Kubo, Matsubae-Yokoyama K, and T. Nagasaka, Magnetic separation of phosphorus enriched phase from multiphase dephosphorization slag, *ISIJ Int.*, 50(2010), No. 1, p. 59.

[14] K. Morita, M.X. Guo, N. Oka, and N. Sano, Resurrection of the iron and phosphorus resource in steel-making slag, *J. Mater. Cycles Waste Manage.*, 4(2002), p. 93.

[15] Z.H. Tian, B.H. Li, X.M. Zhang, and Z.H. Jiang, Double slag operation dephosphorization in BOF for producing low phosphorus steel, *J. Iron Steel Res. Int.*, 16(2009), No. 3, p. 6.

[16] D.R. Gaskell, *Introduction to the Thermodynamics of Materials*, Taylor and Francis, Washington, 1995.